ISIJ International, Vol. 57 (2017), No. 7, pp. 1241–1245

In-situ Heating EBSD Study of Effects of Cold Reduction Ratio on Recrystallization and Grain Growth Behaviors in 3% Si Electrical Steels

Hyunwoo MUN,[1)] Seil LEE[2)] and Yang Moo KOO[1)*]

1) Graduate Institute of Ferrous Technology (GIFT), Pohang University of Science and Technology (POSTECH), Pohang, 790-784 Republic of Korea.
2) Steel Product II Research Group, POSCO Technical Research Laboratories, Pohang, 790-785 Republic of Korea.

(*Received on December 21, 2016; accepted on March 23, 2017*)

Crystallographic texture development during recrystallization in samples cold-rolled to 78, 87 and 96% thickness reduction R were measured using EBSD on an *in-situ* heating stage inside a field emission scanning electron microscope. Nucleation, recrystallization and grain growth of grains having $\{411\}<148>$ orientation occurred intensely and steadily inside the deformed region. Through this phenomenon, grains having $\{411\}<148>$ showed larger average grain sizes than other textures at R = 87% and 96%. Due to the $\{411\}<148>$ texture component, the $\{111\}<112>$ texture component, which is known as a high reduction emerging texture, weakened. At R = 76%, grains having Goss orientation were frequently observed. However, at R = 87% and 96%, the $\{111\}<112>$ and the $\{411\}<148>$ texture components became dominant and the α^* fiber was strengthened.

KEY WORDS: *in situ* EBSD; recrystallization textures; $\{411\}<148>$ orientation.

1. Introduction

Electrical steel, which is used in energy transformation, contains up to 6.5 wt% Si. The Si significantly increases the electrical resistivity of the steel, and as a consequence reduces power loss caused from dissipation as heat or noise. The energy loss in the electrical steel is called 'iron loss', and is composed of hysteresis loss, eddy current loss and anomalous loss. Eddy current loss is proportional to the square of the thickness, so researchers are trying to reduce it.

In general, steel makers increase the cold reduction ratio R to reduce the thickness of the electrical steel. R > 80% applied to body centered cubic (BCC) single-phase steel like ULC steel or IF steel makes $\{111\}<112>$[1)] and $\{411\}<148>$[2)] texture components dominant. However, mechanisms by which proportions of texture components changes and grains grow during recrystallization are not understood in detail.

The magnetic properties of the electrical steels are influenced by their recrystallization texture. In BCC iron the $<100>$ axis is the easiest magnetization direction.[3)] Therefore ND||$<100>$ texture is desirable and $\{100\}<0uv>$ is an ideal texture for non-oriented electrical steel, which is used on the rotating machines such as motors. However, typical non-oriented electrical steels have a texture composed of $\{111\}<112>$, $\{111\}<110>$, $\{112\}<110>$ and $\{110\}<001>$ components. Therefore, magnetic properties of electric steels can be improved by optimizing their textures.

A heating stage that can be used inside a field emission scanning electron microscope (FE-SEM) can used to observe high-temperature phenomena like recrystallization[4–7)] and phase transformation.[8–11)] In this paper, *in-situ* heating EBSD recrystallization was used to study the textures and crystal growth of electrical steel with different R.

2. Experimental

An ingot of a steel that contained 2.8 wt% Si, with small amounts of Al, Mn and other elements (**Table 1**) was heated to 1 200°C and hot-rolled to thickness of 2.3 mm, then cold-rolled to thickness of 0.5, 0.3, or 0.1 mm, which correspond to R = 78, 87 and 96% respectively. Specimens of 7 mm × 5 mm were cut from the cold-rolled sheets for in-situ SEM/EBSD measurement. Before the *in-situ* heating experiment, the surfaces of the specimens were mechanically polished with a final polish in a 1:1 mixture of ethanol and colloidal silica suspension for 30 min.

The heating stage (**Fig. 1**) (TSL Solutions) includes a shield plate that prevents thermal shock to the objective lens

Table 1. Composition of the steel specimen.

Si	Al	Mn	C	S	N	Fe
2.8	0.5	0.3	0.002	0.001	0.002	Balance

* Corresponding author: E-mail: koo@postech.ac.kr
DOI: http://dx.doi.org/10.2355/isijinternational.ISIJINT-2016-564

of the FE-SEM, and a circulating-water cooling system to prevent the device from overheating. Thermocouples are attached to the heater and to the specimen. The temperature of the specimen is controlled by changing the temperature of the heater. Specimen temperatures up to 1 000°C are possible.

The experiments were conducted with a FEI FE-SEM (Quanta 3D FEG) operated at 20-keV accelerating voltage, and 16-nA beam current. The specimens were heated using the heating stage under high vacuum (~10^{-5} torr) in the FE-SEM equipment. The *in-situ* heating was performed stepwise (**Fig. 2**). The annealing time for each step was 10 s and EBSD was measured at 300°C to avoid texture change during measurement.

Optical microscope (OM) images at 200× magnification were captured using an Olympus BX51M on specimens at each reduction after polishing then etching in 5% nital solution.

For EBSD, the step size was fixed to 2 μm. Data were analyzed using a TSL OIM 7.2.1 software. The recrystallized fraction was quantified using the grain orientation spread (GOS) method. The GOS values used previously to distinguish recrystallized grains ranged from < 1° to < 3°.[12–15] In this paper, GOS < 1° was determined to represent recrystallization. The tolerance angle from each orientation was 15° and the fraction of each texture was calculated with the total recrystallized fraction.

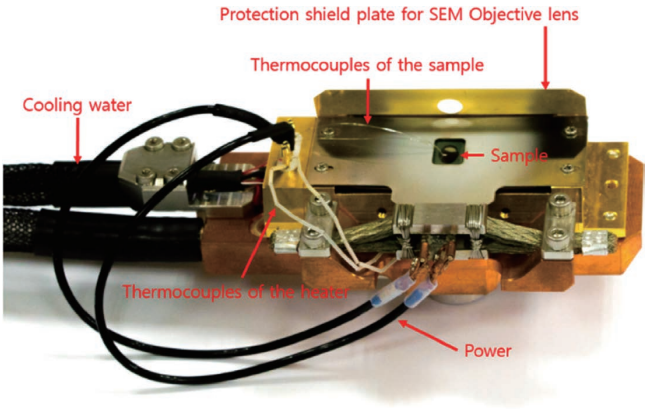

Fig. 1. Heating stage for SEM/EBSD analysis. (Online version in color.)

3. Results and Discussion

The microstructures of cold rolled specimens (**Fig. 3**) changed with R. The area fractions of {111}<112> (**Fig. 4**(a)) and {411}<148> (Fig. 4(b)) texture components were similar, but the area fraction of {111}<112> texture component decreased as annealing temperature increased, whereas {411}<148> texture component increased as annealing temperature increased. The difference between the textures was small at R = 78%, but increased as R increased.

The textures nucleated and their grains grew differently. As a result, the area fraction of texture components except the {411}<148> component decreased during grain growth (Fig. 4). The {411}<148> and the {111}<112>-oriented grains, which retain high area fraction, nucleated consistently, whereas nucleation of other texture components was concentrated during the early stage of annealing in which there are deformed regions (**Fig. 5**. 700°C). For this reason, the area fraction of texture components other than {411}<148> and {111}<112> texture components were low.

Goss texture is a typical texture weakening during annealing. At 700°C, the nucleation rate in the {110} ND plane was fast, and Goss texture was readily nucleated and grew (Fig. 5(a)). However, little nucleation or grain growth by absorbing grains that had different orientations than the Goss oriented grains occurred during further anneal-

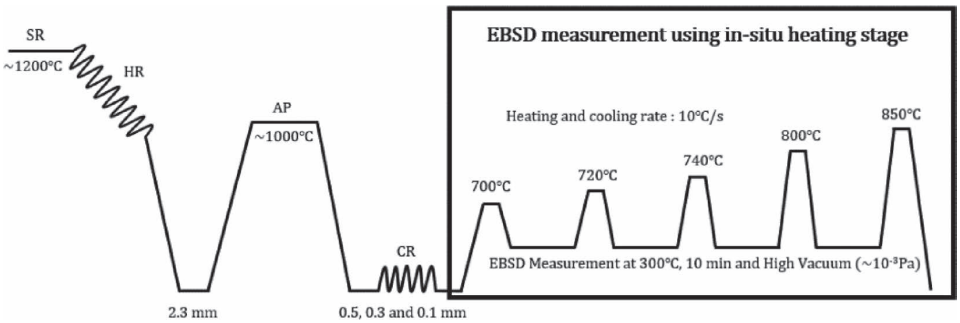

Fig. 2. Sample preparation processes and the heating cycle.

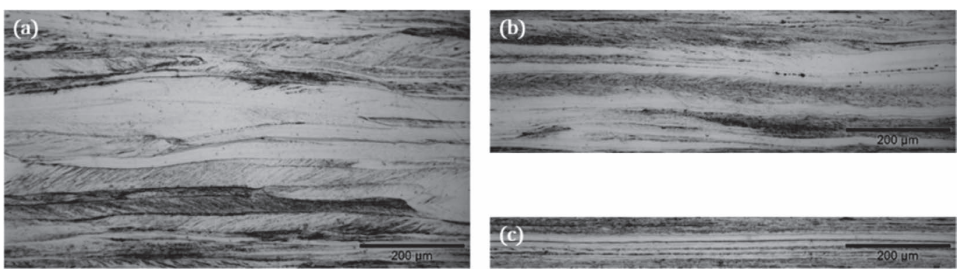

Fig. 3. Transverse-direction section OM images of (a) 78%, (b) 87% and (c) 96% cold-rolled specimens.

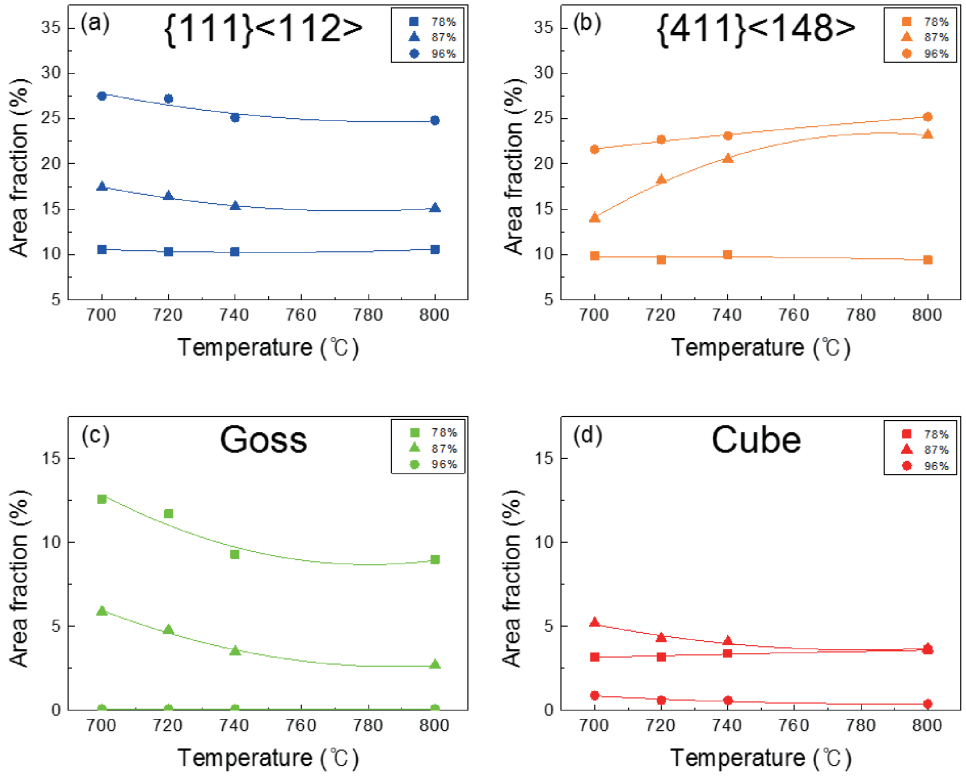

Fig. 4. The Area fraction of textures with different reduction ratios during annealing. (Online version in color.)

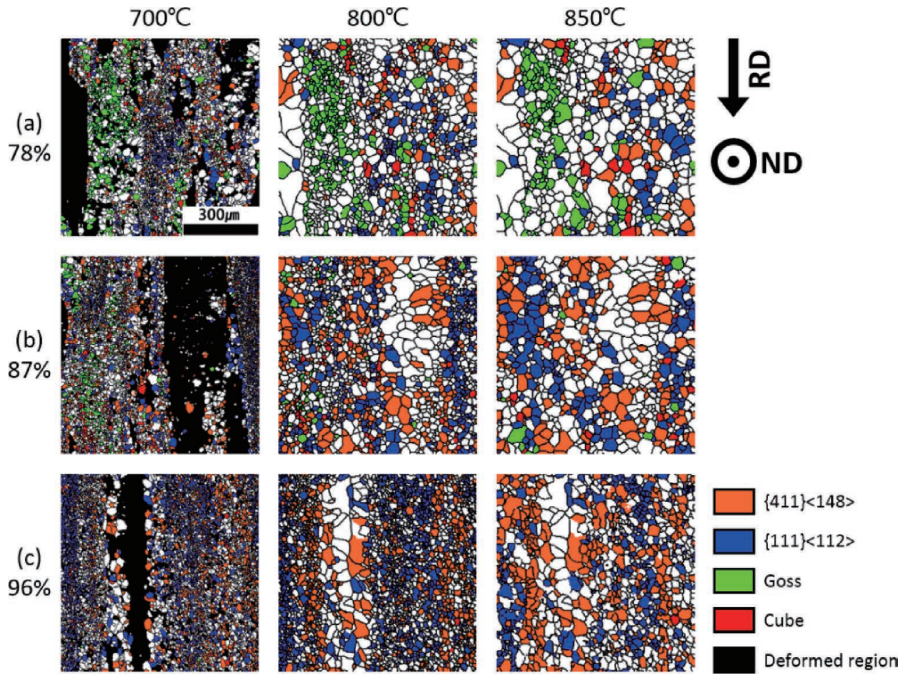

Fig. 5. Orientation maps of the specimens with the reduction (a) 78%, (b) 87% and (c) 96% at the temperature 700°C, 800°C and 850°C. (Online version in color.)

ing. Other texture components developed in the deformed region, so the recrystallized Goss fraction in the whole recrystallized grain decreased. Most Goss-oriented grains occurred in a region in which numerous grains with Goss orientation were gathered together (Fig. 5(a)). They nucleated together and persisted inside the Goss-concentrated region. The size of this region changed little during grain growth, but the size of the grains increased; the reason is that grain boundaries inside the Goss-concentrated region have low angles, so Goss grains grow by merging with other Goss grains. However, because of the low-angle boundaries, the grains grow slowly.

The area fraction of Goss-oriented grains drastically decreased as R increased, and few such grains were observed at R = 96%. Unlike other grains, the Goss grain size decreased (**Fig. 6**(c)) due to absorption of Goss grains. Because Goss grains were rare at R = 96%, they were easily eliminated by being absorbed by other grains.

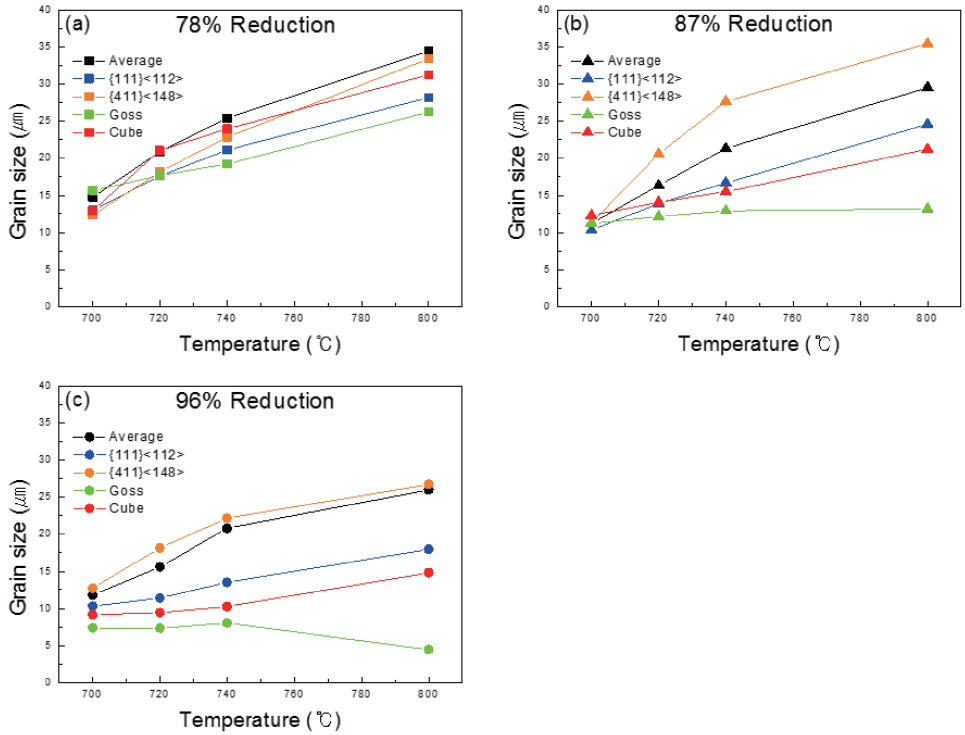

Fig. 6. The Grain size of textures with different reduction ratio during annealing. (Online version in color.)

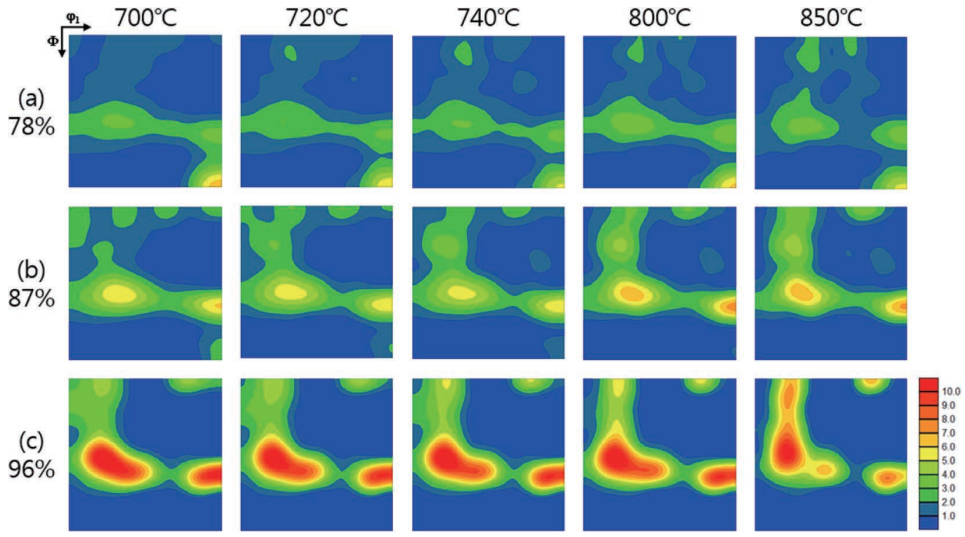

Fig. 7. ODF maps **(φ_2 = 45° section)** of specimens with reduction ratio (a) 78%, (b) 87% and (c) 96% at various temperatures. (Online version in color.)

Generally, high R yielded small grain size; the only exception was {411}<148> texture; these grains were larger at 87% R (740°C, 28 μm) than at R = 78% (740°C, 23 μm). At R = 87%, this component grew rapidly during annealing; this observation suggests that R = 87% is near the optimal R for the growth of {411}<148>-oriented grains.

Compared to the average grain size regardless of texture components, the average grain size of {411}<148>-oriented grains was larger at R = 87% or 96% and the only texture component in which grains were larger than average at high R. This result suggests that growth of {411}<148>-oriented grains requires high R.

R also affected grain sizes very differently. The grain sizes of most texture components were similar at R = 78% (Fig. 6(a)), but Goss and cube grain sizes decreased at R = 87% and 96%.

The intensity of the {411}<148> texture component is increased on the ODF maps (**Fig. 7**). This texture component increased as R increased. Because of the growth of {411}<148> texture component, the α^* fiber component (Fig. 7) intensified in the ODF maps at R = 87% and 96%.

Recrystallization and grain growth of the {111}<112>-oriented grains also changed drastically as R increased. This texture change is expressed as γ fiber strengthening on ODF maps. The overall recrystallization and grain growth phenomena resemble that of general steel materials.

The location of maximum intensity on the ODF (Fig. 7) at 850°C at R = 96% had slightly lower Φ value than that of {111}<112> texture component; the reason is that as annealing progressed, the proportion of {411}<148>

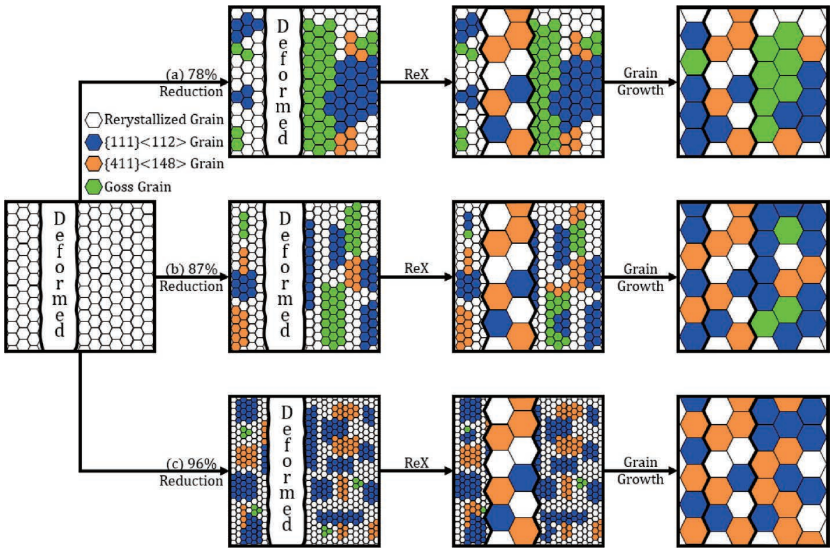

Fig. 9. The schematic diagram of the specimens with the reduction (a) 78%, (b) 87% and (c) 96% at various temperatures. (Online version in color.)

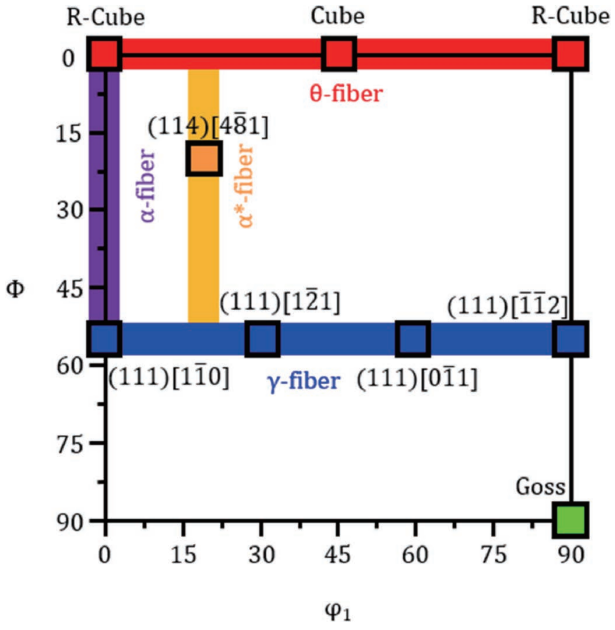

Fig. 8. ODF orientation map. (Online version in color.)

texture component increased while the proportion of the {111}<112> texture component decreased (Fig. 4). This phenomenon reinforces α^* fiber. Also, the texture near the cube orientation developed by {411}<148> texture component strengthening.

Change in R was associated with several phenomena (**Fig. 9**). The recrystallized grain size decreased as R increased. The textures developed differed with R: at R, = 78% the recrystallization of the Goss texture was prevalent and the grains with orientation near the Goss texture emerged together. They maintained the low angle boundaries to each other and grew up by absorbing themselves. At high R, the {111}<112> and {411}<148> texture components became dominant. The grain size of the {411}<148> texture component was especially large due to the active recrystallization at the deformed region.

4. Conclusion

Textures that develop during cold rolling to R = 78, 87 and 96% thickness reduction were investigated using in-situ heating in an FE-SEM. At high R, the {411}<148> component was the only texture in which grain size exceeded the average grain size . This result occurred because nucleation, recrystallization and grain growth of {411}<148>-oriented grains occurred steadily inside the deformed region. R affected recrystallization textures. As R increased, the {111}<112> and the {411}<148> texture components became dominant. The proportion of Goss and the other textures like the Cube decreased due to the growth of {411}<148> and {111}<112>-oriented grains. The α^* fiber component was strengthened in the overall textures on the ODF maps as R increased; this result was also a consequence of growth of {411}<148>oriented grains.

REFERENCES

1) M. Holscher, D. Raabe and K. Lucke: *Steel Res.*, **62** (1991), 567.
2) H. Homma, S. Nakamura and N. Yoshinaga: *Mater. Sci. Forum*, **467** (2004), 269.
3) B. D. Cullity and C. D. Graham: Introduction to Magnetic Materials, 2nd Ed., Wiley, Hoboken, NJ, (2008), 199.
4) M. Bestmann, S. Piazolo, C. J. Spiers and D. J. Prior: *J. Struct. Geol.*, **27** (2005), 447.
5) H. Nakamichi, F. Humphreys and I. Brough: *J. Microsc.*, **230** (2008), 464.
6) J.-H. Kim, D.-I. Kim, J. S. Kim, S.-H. Choi, K.-W. Yi and K. H. Oh: *Appl. Microsc.*, **43** (2013), 88.
7) D.-I. Kim, J. Kim, J. Kim and S.-H. Choi: *Acta Mater.*, **68** (2014), 9.
8) N. Yoshinaga, L. Kestens and B. C. De Cooman: *Mater. Sci. Forum*, **495** (2005), 1267.
9) I. Lischewski, D. Kirch, A. Ziemons and G. Gottstein: *Texture, Stress, Microstruct.*, **2008** (2008), DOI: http://dx.doi.org/10.1155/2008/294508
10) T. Fukino and S. Tsurekawa: *Mater. Trans.*, **49** (2008), 2770.
11) S. Clark, V. Janik, A. Rijkenberg and S. Sridhar: *Mater. Charact.*, **115** (2016), 83.
12) M. H. Alvi, S. Cheong, H. Weiland and A. D. Rollett: Proc. 1st Int. Symp. on Metallurgical Modeling for Aluminum Alloys, ASM lintternational, Materials Park, OH, (2003), 191.
13) S. Mitsche, C. Sommitsch and P. Polt: *Sonderbd Prakt Metallogr*, **38** (2006), 43.
14) S. W. Cheong and H. Weiland: *Mater. Sci. Forum*, **558** (2007), 153.
15) S. Abolghasem, S. Basu and M. R. Shankar: *J. Mater. Res.*, **28** (2013), 2056.